The characteristics of salt fingers in a variety of fluid systems, including stellar interiors, liquid metals, oceans, and magmas

Raymond W. Schmitt

The characteristics of salt fingers in a variety of fluid systems, including stellar interiors, liquid metals, oceans, and magmas

Raymond W. Schmitt

Woods Hole Oceanographic Institution, Woods Hole, Massachusetts 02543

The growth rates, flux ratios, wavenumbers, and bandwidths of salt fingers are computed for Prandtl numbers from 10^{-7} to 10^4 and diffusivity ratios from 1 to 10^8, using the exact similarity solutions of Schmitt [Deep-Sea Res. **26A**, 23 (1979)]. This model successfully explains the variation in flux ratio in the heat/salt and salt/sugar systems and produces salt-finger spectra in agreement with ocean observations. The calculations presented here should be useful in the study of double diffusion in astrophysics, chemistry, geology, metallurgy, meteorology, and oceanography, and may be applicable to problems in the growth of semiconductor crystals.

I. INTRODUCTION

The double-diffusive processes depend on the difference between the diffusivities of two density-affecting components to release the potential energy available in an unstable distribution of one component. If the slower-diffusing component has the unstable distribution, with the overall stratification remaining stable, then the structures realized are the tall, narrow convective cells known as salt fingers.[1] If the faster-diffusing substance has the unstable distribution, then diffusive interfaces are formed, across which the diffusion of the more mobile component drives convective motions in adjacent layers.[2]

The qualitative effects of double-diffusive mixing, layer generation, and the formation of tall, narrow salt fingers, are well known for the ocean and have recently been recognized in magmas,[3] the atmosphere,[4] stars,[5] liquid metals,[6] and semiconductors.[7] However, quantitative data on transport rates, flux ratios, and the scales of the instabilities are generally lacking, save for the oceanographic heat/salt system and the laboratory salt/sugar system. There exists a simple theory that successfully predicts the flux ratio and wavenumber of the salt-finger instability in these two systems, where both the Prandtl number and diffusivity ratio vary by two orders of magnitude. In the following sections, the calculations of the finger growth rate, flux ratio, wavenumber, and bandwidth are extended to other parameter ranges. This should be especially helpful in those systems where experimental observations of the active process are particularly hard to obtain (e.g., magmas, stars).

II. THE FINGER MODEL

The model we will use is that given by Schmitt,[8] which is an extension to all Prandtl numbers and diffusivity ratios of the treatment developed by Stern.[9] We model the fingers as exponentially growing perturbations in T (faster-diffusing component, diffusivity $= K_T$), S (slower-diffusing component, diffusivity $= K_S$), and W (vertical velocity), with sinusoidal variations in both horizontal directions. The vertical density gradients due to T and S are uniform and constant, since the fingers are not assumed to interact with the basic state. These gradients are given by $\overline{\alpha T_z}$ and $\overline{\beta S_z}$, where $\alpha = -(1/\rho)(\partial\rho/\partial T), \beta = (1/\rho)(\partial\rho/\partial S), \rho = $ density, and z is positive upward. The net vertical density gradient is stable (negative), given by $\rho_z = \beta S_z - \alpha T_z$, since $\alpha T_z > \beta S_z$. The similarity solutions to the Boussinesq conservation equations in an unbounded fluid have the form $(T', S', W') = (\hat{T}, \hat{S}, \hat{W}) e^{\lambda t} \sin(m_1 x) \sin(m_2 y)$. The growth rate λ is given by

$$\lambda = (g \, \overline{\alpha T_z})^{1/2} \, G(R, \gamma, \tau, \sigma), \tag{1}$$

and the total horizontal wavenumber is

$$(m_1^2 + m_2^2)^{1/2} = (g \, \overline{\alpha T_z}/\nu K_T)^{1/4} \, M(R, \gamma, \tau, \sigma), \tag{2}$$

where the density ratio $R = (\overline{\alpha T_z}/\overline{\beta S_z})$ $(1 \leqslant R \leqslant \tau)$, the flux ratio $\gamma = (\alpha T'/\beta S')$ $(0 < \gamma \leqslant 1)$, the Prandtl number $\sigma = \nu/K_T$, and the diffusivity ratio (Lewis number), $\tau = K_T/K_S$. The dimensionless growth rate is

$$G = (\tau\gamma - R) \left(\frac{(1-\gamma)}{\gamma R (\tau - 1)[R (\sigma\tau - 1) - \tau\gamma(\sigma - 1)]} \right)^{1/2}, \tag{3}$$

and the dimensionless wavenumber is

$$M = (R - \gamma)^{1/2} \tau^{1/2}$$
$$\times \left(\frac{\sigma(1 - \gamma)}{\gamma R (\tau - 1)[R (\sigma\tau - 1) - \tau\gamma(\sigma - 1)]} \right)^{1/4}. \tag{4}$$

We expect the dominant fingers to be those with a flux ratio (γ_m) which maximizes the growth rate. Taking $a = (\sigma - 1)$, $b = (\sigma + 1 - 2\sigma\tau) R /\tau$, $c = (\sigma\tau + 1 - 2\sigma) R /\tau$, $d = (\sigma\tau - 1) R^2/\tau^2$, $H = (3ac - b^2)/9a^2$, $K = (2b^3 - 9abc + 27a^2d)/27a^3$, and $\theta = \frac{1}{3} \arccos [-K/2(-H)^{3/2}]$, we find that

$$\gamma_m = (R /\tau)^{1/2}, \qquad \text{for } \sigma = 0,$$
$$\gamma_m = 2(-H)^{1/2} \cos \theta - b /3a, \qquad \text{for } 0 < \sigma < 1,$$
$$\gamma_m = \frac{1}{2}(\frac{1}{4} + 2R /\tau)^{1/2} + \frac{1}{4}, \qquad \text{for } \sigma = 1,$$
$$\gamma_m = 2(-H)^{1/2} \cos(\theta + 4\pi/3) - b /3a, \qquad \text{for } \sigma > 1.$$
$$\tag{5}$$

These relationships are valid for all σ and $\tau (> 1)$, but have been evaluated only for the heat/salt $(\sigma = 7, \tau = 10^2)$ and salt/sugar $(\sigma = 10^3, \tau = 3)$ cases. Here we examine the vari-

ation of G, γ_m, M, and a measure of the finger bandwidth, Q, over a wider area of the σ, τ plane.

III. THE FINGER GROWTH RATE

A contour plot of the nondimensional growth rate G, evaluated at $\gamma = \gamma_m$, and a density ratio of 1 (giving the maximum growth rate possible) for σ from 10^{-7} to 10^4 and τ from 1 to 10^8, is given in Fig. 1(a). The regions of the σ, τ plane occupied by a number of fluid systems are indicated. Note that the fastest-growing fingers occur at low Prandtl number and high diffusivity ratio. In the limit of large τ and $\sigma \to 0$, such that $\sigma\tau \to 0$, the growth rate approaches unity. Such conditions are found in stellar interiors, liquid metals, and metallic semiconductors. We can also see that the

GROWTH RATE, G
(a) $R = 10$

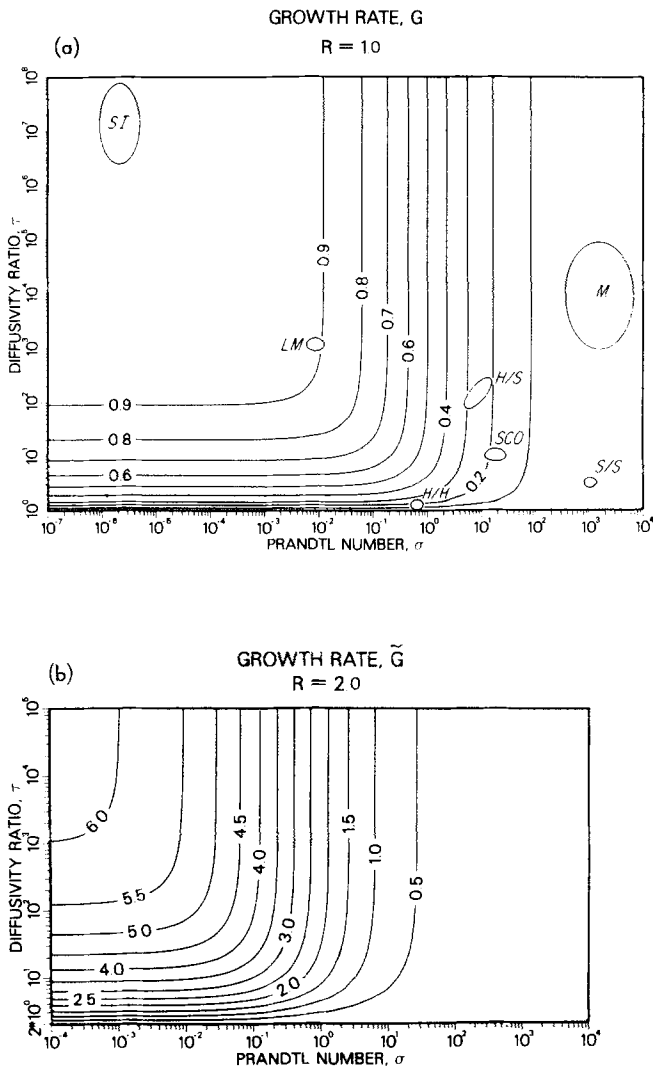GROWTH RATE, $\tilde{G}$
(b) $R = 2\,0$

FIG. 1. The finger growth rate. (a) The nondimensional growth rate G, of the fastest-growing salt finger at a density ratio of 1 for $10^{-7} < \sigma < 10^4$ and $1 < \tau < 10^8$. The areas of the σ, τ plane occupied by a number of double-diffusive systems are indicated. SI = stellar interiors (Ref. 6), LM = liquid metals (Ref. 7), and metallic semiconductors, (Ref. 8), H/S = heat/salt, SCO = semiconductor oxides (Ref. 8), H/H = humidity/heat (Ref. 5), S/S = salt/sugar, and M = magmas (Ref. 4). (b) The finger growth rate $\tilde{G}$, in e foldings per buoyancy period, at $R = 2$ for $10^{-4} < \sigma < 10^4$ and $2 < \tau < 10^5$.

slowest growth rates are to be found at high σ and low τ, for instance, the salt/sugar case. It is important to keep the differences between the growth rates of fingers in these various systems firmly in mind when trying to draw analogies. This is especially so if the finger response to other dynamical processes such as internal waves or shear instability is being considered.

In this regard it is useful to rescale the growth rate with the local Brünt–Väisälä or buoyancy period, in order to directly compare the finger time scales with those of other processes in a stratified fluid. This is accomplished by the transformation: $\tilde{G} = 2\pi G /(1 - R^{-1})^{1/2}$, which yields the growth rate in e foldings per buoyancy period. Such scaling can be applied only when the density ratio is greater than 1, since there is no density stratification at $R = 1$. A convenient density ratio to use is $R = 2$. At that value the potential energy in the unstable distribution of the slower-diffusing substance is one-half the maximum value that can be supported by the distribution of the more mobile component. The potential energy at $R = 2$ is also equal to the energy required to mix the density field to uniformity over a vertical interval with uniform gradients.[10]

A contour plot of $\tilde{G}$ in the σ, τ plane is given in Fig. 1(b). (Note that τ now begins at 2, since uniformly stratified systems with $\tau < R$ will not form fingers.) This scaling clearly reveals that some systems have finger e-folding times that are shorter than the time scale of internal waves and therefore might be regarded as vigorous (stellar interiors, liquid metals and semiconductors, heat/salt). In these fluids we predict that the fingers will compete successfully with the processes of internal wave breaking and shear instability which are found in a geophysical setting, if not in the laboratory. Note also that there will always be some R, sufficiently close to 1, at which the finger e-folding time becomes less than the buoyancy period, even for the sluggish systems (salt/sugar, magmas), because the buoyancy period $\to \infty$ as $R \to 1$.

IV. THE FLUX RATIO

Perhaps the most important and most easily measured parameter in salt-finger experiments is the flux ratio γ. It is defined as the absolute value of the ratio of the convective flux of the faster-diffusing component (heat) to the convective flux of the slower-diffusing component (salt). Measured values of γ are in excellent agreement with γ_m given by Eq. (5) in the heat/salt system, where $\gamma \simeq 0.57$[11] to 0.70,[12] and in the salt/sugar system where $\gamma \simeq 0.90$.[13] Recent and more accurate data in the salt/sugar system[14] show that variations in γ with R are well explained by this model. Given the two-orders-of-magnitude variation in σ and τ represented by these cases, it seems likely that γ_m, as given by Eq. (5), will be a good indicator of the flux ratio in other parts of the σ, τ plane as well. Accordingly, a contour plot of γ_m as a function of σ and τ for $R = 2$ is presented in Fig. 2. (The state of $R = 1$ is experimentally difficult to approach, and we set $R = 2$ in further computations as well.)

Figure 2 reveals that γ_m is largely a function of τ, being highest at low τ, but is also dependent on σ, getting small at low σ. This is certainly reasonable, since the high thermal diffusivities at low σ and high τ would act to nearly eliminate

Raymond W. Schmitt   2374
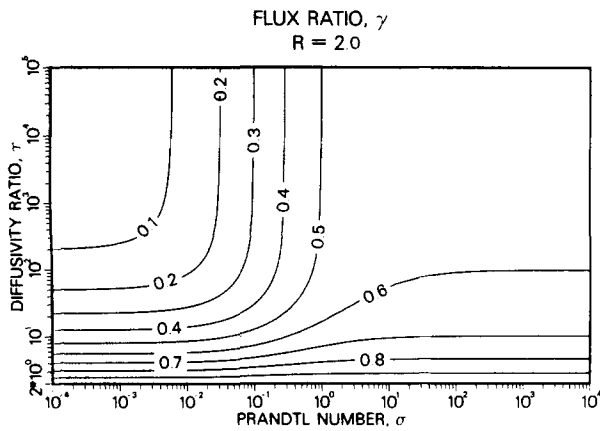
FLUX RATIO, γ
$R = 2.0$

FIG. 2. The flux ratio of the fastest growing salt finger at $R = 2$, for $10^{-4} < \sigma < 10^4$ and $2 < \tau < 10^5$.

the thermal contrast between up- and down-going fingers so that very little heat could be carried convectively. We also see that for $\tau > 10$ and $\sigma > 1$, the flux ratio falls between 0.5 and 0.7 at $R = 2$. As R approaches 1, Eq. (5) reveals that γ_m increases for systems with $\sigma > 1$; $\gamma_m = \frac{1}{2}$ when $\sigma = 1$; and γ_m decreases in those cases where $\sigma < 1$. Figure 2 should be useful to those exploring new parameter ranges. It will be especially interesting to see if additional experimental data agree with the theoretical prediction.

V. THE FINGER WAVENUMBER AND BANDWIDTH

Laboratory experiments[15] to date have supported the dependence of the salt-finger wavenumber on the $\frac{1}{4}$ power of the vertical temperature gradient. Some experiments[16] seem to suggest that the equilibrium or nongrowing finger is the most often found, while observations in the ocean[17,18] are much more consistent with the fastest-growing finger, which has a lower wavenumber. However, the oceanic data also indicate that the fingers can be somewhat broadbanded, with significant energy in a range of wavenumbers about the fastest growing. We here present calculations of the dimensionless wavenumber M and a bandwidth parameter, Q.

Figure 3(a) is a contour plot of $M(\gamma_m)$ in the σ, τ plane, for $R = 2$. We see that over much of the parameter space, M is between 0.6 and 0.9. The thinnest fingers (highest M) are found at high τ and low σ; while the thickest fingers (low M) are found when both τ and σ are low. We expect that the dominant wavenumber will be given by the fastest-growing finger, but we must realize that in many cases the maximization of G is not strongly selective. That is, there exists a range of wavenumbers which have high growth rates, and we need some measure of the bandwidth of the process.

A traditional measure of bandwidth is the Q of a system, defined as the center frequency divided by the $\frac{1}{2}$-power bandwidth. In order to compute a wavenumber spectrum for growing salt fingers, one must specify an input spectrum and the length of time the fingers grow; thus, the choice of a definition of Q is somewhat arbitrary. For the present purposes we will assume that the fingers evolve from a "white noise" spectrum for the time it takes the fastest-growing finger to e fold in amplitude. Since the horizontal wavenumber spectrum (of T, for instance) is proportional to $\exp(2\lambda t)$, and

(a) WAVENUMBER, M
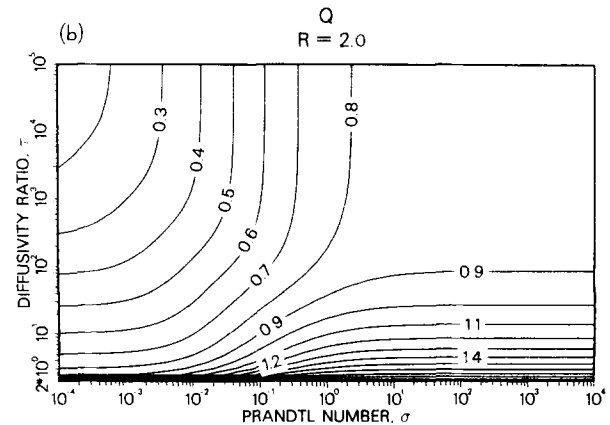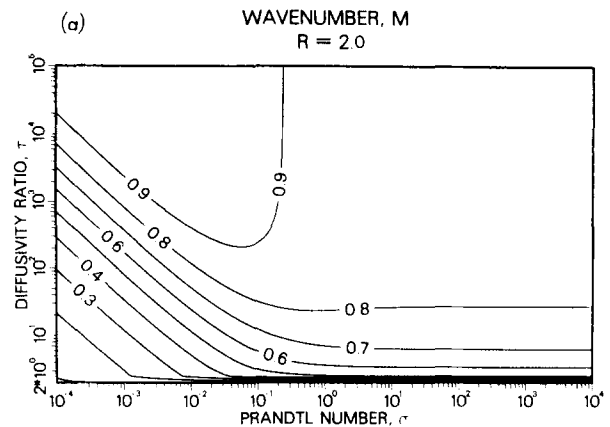$R = 2.0$

(b) Q
$R = 2.0$

FIG. 3. The finger wavenumber and bandwidth. (a) Contours of the nondimensional wavenumber M of the fastest-growing finger at $R = 2$, for $10^{-4} < \sigma < 10^4$ and $2 < \tau < 10^5$. (b) Contours of the bandwidth parameter Q at $R = 2$, for $10^{-4} < \sigma < 10^4$ and $2 < \tau < 10^5$. The definition of Q is given in the text. These low Q's indicate that fingers are a fairly broadband process, especially in the early stages of growth.

we choose $t = 1/\lambda_m$ (where λ_m = maximum growth rate), we must find the wavenumbers M_u and M_l which have the growth rates satisfying $\exp(2\lambda/\lambda_m) = \frac{1}{2} e^2 = 3.695$. The two wavenumbers which satisfy this relation have a growth rate equal to 0.653 times the maximum growth rate and are readily found using an iterative technique. With ΔM being the difference between these two wavenumbers, and M_m being the wavenumber of the fastest-growing finger, our bandwidth parameter is given by $Q = M_m/\Delta M$. Contours of Q in the σ, τ plane are shown in Fig. 3(b), for the case of $R = 2$.

Here Q is seen to be less than 1 in most of the parameter range of interest. Only in the low-τ, high-σ region does it exceed unity. These low Q's indicate that, at least in the early stages of growth, salt fingers are a very broadband process. Given more time, of course, the fastest-growing finger becomes more dominant; Q is typically about 3 if the fingers grow for ten e-folding periods. Figure 3(b) shows that the fast-growing, low-flux-ratio fingers found at low σ and high τ also have the lowest Q. This indicates that considerable variation in flux ratio and wavenumber is to be expected in these systems; indeed, the fingers may have some of the characteristics of turbulence.

TABLE I. The Prandtl number (σ), diffusivity ratio (τ), and R * (the density ratio at which $\tilde{G} = 1$) for a number of double-diffusive systems. Also given are G, $\tilde{G}$, γ_m, M, and Q for $R = 1$ and $R = 2$.

System	σ	τ	R *	R	G	$\tilde{G}$	γ_m	M	Q
Stellar	$\sim 2 \times 10^{-6}$	0.2–0.7×10^7	40	1	1.00	. . .	0.002	0.94	0.05
interiors				2	0.71	6.27	0.002	1.00	0.05
Liquid metals and metallic semiconductors	$\sim 10^{-2}$	10^3	17	1	0.90	. . .	0.10	0.92	0.33
				2	0.61	5.43	0.13	0.94	0.41
Heat/salt									
30 °C	5.5	85	2.04	1	0.30	. . .	0.71	0.54	0.50
				2	0.12	1.03	0.58	0.83	0.88
0 °C	13	215	1.65	1	0.22	. . .	0.79	0.46	0.44
				2	0.08	0.70	0.58	0.84	0.86
Oxide semiconductors	~ 10	10–20	1.6	1	0.23	. . .	0.79	0.47	0.50
				2	0.07–0.08	0.59–0.69	0.64–0.69	0.74–0.79	1.03–1.16
Humidity/heat	0.6	1.2	1.11	1	0.18	. . .	0.94	0.29	0.70
Salt/sugar	10^3	3	1.02	1	0.025	. . .	0.98	0.15	0.22
				2	0.002	0.018	0.89	0.57	1.60
Magmas	0.4–5×10^3	10^3–10^5	1.007–	1	0.01–0.05	. . .	0.95–0.99	0.12–0.22	0.13–0.23
			1.06	2	0.004–0.015	0.04–0.13	0.59	0.84	0.84

VI. SUMMARY

This examination of the growth rate, flux ratio, wavenumber, and bandwidth of the fastest-growing salt finger over a wide range in Prandtl number and diffusivity ratio has shown that:

(1) The systems with the highest growth rates are those with low Prandtl number and high diffusivity ratio.

(2) Systems with low σ and high τ are predicted to have low flux ratios (0.1–0.2) while other systems with $\sigma > 1$ and $\tau > 10$ should have γ_m between 0.5 and 0.7 at a density ratio of 2.

(3) Except for a region of low σ and low τ the nondimensional wavenumber of the fastest-growing finger lies between 0.6 and 1.0 for $R = 2$.

(4) The bandwidth of a horizontal wavenumber spectrum grown from "white noise" for one e folding of the fastest-growing finger is typically of the same order as the central wavenumber, for $\sigma > 1$, $\tau > 10$, and $R \simeq 2$. (That is, if the fastest-growing finger has a wavenumber of one cycle per centimeter, then significant energy should be found for wavenumbers between 0.5 and 1.5 cycles per centimeter.) The bandwidth becomes much larger, five to ten times the peak wavenumber, for small σ and large τ.

For several double-diffusive systems of current interest, the values of G, $\tilde{G}$, γ_m, M, and Q have been compiled for $R = 1$ and $R = 2$ in Table I. Also given is the density ratio $(R \, *)$ for which $\tilde{G} = 1$. Significant changes in the intensity of salt-finger convection appear to occur when $\tilde{G} = 1$ in the ocean.[19] This may indicate a transition from finger-dominated mixing to internal-wave-dominated mixing as R increases past R *, and could be occurring in other geophysical systems as well. The table shows that stellar interiors, the liquid metals, and semiconductors, and the warm (30 °C) heat/salt systems have growth rates in excess of one e folding per buoyancy period at $R = 2$, and may be regarded as vigorous. At the other extreme, the salt/sugar and magma systems are much slower, taking 7–55 buoyancy periods to e fold in amplitude, and can be regarded as sluggish.

Since this model has been so successful at explaining variations in the flux ratio in the heat/salt and salt/sugar systems, and in interpreting the spectrum of oceanic salt fingers, these calculations should prove useful to those studying other systems. Equations (1)–(5) can be employed to draw analogies between systems, to analyze data from new laboratory experiments, and to construct models in those situations where data is unobtainable. Problems that can benefit from this analysis include the interaction of salt fingers with internal waves and the study of fingers formed in alloys, semiconductors, and magmas cooled from below. It will be especially interesting to see if the low flux ratios predicted for the liquid metal systems are observed experimentally.

ACKNOWLEDGMENT

[1] M. E. Stern, Tellus 12, 172 (1960).
[2] J. S. Turner, Int. J. Heat Mass Transfer 8, 759 (1965).
[3] H. E. Huppert and R. S. J. Sparks, Contrib. Mineral. Petrol. 75, 279 (1980).
[4] F. J. Merceret, Boundary-Layer Meteorol. 11, 121 (1977).
[5] R. K. Ulrich, Astrophys. J. 172, 165 (1972).
[6] S. M. Copley, A. F. Giamei, S. M. Johnson, and M. F. Hornbecker, Metallurgical Transactions 1, 2193 (1970).
[7] R. Brown (personal communication, 1983).
[8] R. W. Schmitt, Deep-Sea Res. 26A, 23 (1979).
[9] M. E. Stern, Ocean Circulation Physics (Academic, New York, 1975), p. 191.

[10]R. W. Schmitt and D. T. Georgi, J. Marine Res. **40**, 659 (1982).

[11]J. S. Turner, Deep-Sea Res. **14**, 599 (1979).

[12]R. W. Schmitt, J. Marine Res. **37(3)**, 419 (1979).

[13]R. B. Lambert and J. W. Demenkow, J. Fluid Mech. **54**, 627 (1972).

[14]R. W. Griffiths and B. R. Ruddick, J. Fluid Mech. **99(1)**, 85 (1980).

[15]P. F. Linden, Deep-Sea Res. **20**, 325 (1973).

[16]H. E. Huppert and P. F. Linden, Deep-Sea Res. **23**, 909 (1976).

[17]B. Magnell, J. Phys. Oceanogr. **6**, 511 (1976).

[18]A. E. Gargett and R. W. Schmitt, J. Geophys. Res. **87**, 8017 (1982).

[19]R. W. Schmitt, J. Phys. Oceanogr. **11**, 1015 (1981).